

jugated rgp120 and was found to be comparable to rgp120-GalCer binding (see supplementary material). To demonstrate that the observed interaction is specific, compound **2** and a series of related derivatives (**10-12**, Table I) were tested for their inhibitory activity against rgp120-GalCer binding using a high-performance thin-layer chromatography (HPTLC) competition binding assay.^{3,4} Rgp120 was preincubated with increasing concentrations of each of the compounds shown in Table I, and the solutions were then incubated with GalCer immobilized on HPTLC plates. Inhibition of rgp120-GalCer binding by compounds **2** and **10-13** was quantified by measuring a decrease in the level of bound rgp120. Table I shows the degree of inhibition by 1 mg/mL solutions of the test compounds, as well as concentrations required for 50% inhibition (IC₅₀) for compounds that block rgp120-GalCer binding at micromolar concentrations.

Compound **2** (entry 1) has the highest affinity for rgp120 (IC₅₀ = 120 μM) and competes slightly better than the soluble O-linked glycolipid psychosine hydrochloride (**13**, IC₅₀ = 160 μM, entry 5).¹² Both psychosine and compound **2** exhibit almost complete inhibition of rgp120-GalCer binding (85-100%) at a concentration of 1 mg/mL. A dramatic reduction in inhibitory activity is seen when the length of the hydrocarbon tail is decreased. Compound **10** (entry 2), which contains a C₄ tail, inhibits rgp120-GalCer binding by only 34% at a concentration of 3 mM (1 mg/mL), whereas compounds **11** and **12** (entries 3 and 4) show no inhibitory activity at all, even at concentrations above 3 mM.

The GalCer binding site on gp120 tolerates substitution of a C-glycoside for the O-glycoside as well as substitution of an alkyl amide for the allylic alcohol and hydrocarbon tail of sphingosine. The slightly increased inhibitory activity of compound **2** relative to psychosine (**13**) may arise from the hydrophobicity (poor solvation) of the C-glycosyl linkage relative to the O-glycosyl linkage.¹³ Interestingly, the fatty acid group can be removed altogether from the C-2' position of GalCer (affording psychosine) without a significant loss in gp120 binding activity, despite an obvious reduction in the hydrophobicity of the molecule.⁴ Compound **2** also lacks the C-2' fatty acid and still binds to gp120. Shortening the hydrocarbon tail of compound **2** results in a drastic reduction in inhibitory activity (compare entries 1 and 2), and conversion of the butyl amide to the alcohol (entry 3) or methyl ester (entry 4) completely eliminates binding activity. The rigid amide linkage of compounds **2** and **10** (entries 1 and 2) is positioned similarly to the allylic alcohol of sphingosine and may be a key structural element for gp120 recognition.

In summary, we have designed water-soluble, C-linked galactosphingolipid analogs that block the interaction of recombinant HIV-1 gp120 with GalCer. Given the growing body of evidence suggesting a role for the gp120-GalCer interaction in viral entry, these compounds represent potential inhibitors of the first step in the infection process. Furthermore, determination of the structural elements required for gp120 recognition allows modification of these compounds for receptor-mediated immunology.^{14,15} We are currently investigating these possibilities.

Acknowledgment. Recombinant gp120 and anti-gp120 antibodies were gifts from Dr. Raymond Sweet at SmithKline Beecham (King of Prussia, PA). M.D.B. thanks the American Cancer Society, Proctor & Gamble, and Eli Lilly for Junior Investigator Awards. C.R.B. thanks the ACS Division of Medicinal Chemistry for a graduate fellowship and AT&T Bell Laboratories for a GRPW grant. This research was supported by National Institutes of Health Awards R29 GM43037-02, NS-27405, and NS-31067.

(12) The competition between glycolipids in solution and glycolipids on HPTLC plates for rgp120 binding is not necessarily an equilibrium process under these conditions. Therefore, these values do not represent true solution binding affinities and cannot be considered *K_d* values. However, the concentrations required to inhibit rgp120 binding to immobilized GalCer provide a qualitative measurement of the relative binding affinities for rgp120.

(13) Similar results have been observed in the binding of C-glycosyl mannositides to type 1 *Escherichia coli* mannose-specific receptors (ref 7k).

(14) Bertozzi, C. R.; Bednarski, M. D. *J. Am. Chem. Soc.* 1992, 114, 2242.

(15) Bertozzi, C. R.; Bednarski, M. D. *J. Am. Chem. Soc.* 1992, 114, 5543.

Supplementary Material Available: Experimental details and spectral and analytical data for compounds **2** and **5-12** and all synthetic intermediates and experimental details and results for ELISA and HPTLC binding assays (14 pages). Ordering information is given on any current masthead page.

Topological Rearrangement within a Single Crystal from a Honeycomb [Cd(CN)₂]_n 3D Net to a Diamond Net

B. F. Abrahams,[†] M. J. Hardie,[†] B. F. Hoskins,[†]
R. Robson,^{*,†} and G. A. Williams[†]

School of Chemistry, Inorganic Section
University of Melbourne, Parkville
Victoria, 3052, Australia
Australian Radiation Laboratory
Lower Plenty Road, Yallambie
Victoria, 3085, Australia

Received July 7, 1992

A veritable cornucopia of interesting structural chemistry is provided by cadmium cyanide and its derivatives. The parent itself consists of two completely independent but interpenetrating diamond-related frameworks,¹ while certain derivatives, as Iwamoto has shown, possess single, non-interpenetrating diamond structures² and others show a variety of 2D and 3D structures.³ We report here a remarkable single crystal to single crystal transformation in which an infinite 3D [Cd(CN)₂]_n net undergoes extensive topological change.

When recrystallized from aqueous *tert*-butyl alcohol, cadmium cyanide yields Cd(CN)₂·²/₃H₂O·*t*-BuOH with the infinite 3D honeycomb-like [Cd(CN)₂]_n framework shown in Figure 1.^{3a} These crystals are stable in contact with 50% aqueous *tert*-butyl alcohol or, while free of liquid, in an atmosphere saturated with the vapors of water and *tert*-butyl alcohol, but they degenerate on exposure to air as a result of solvent loss, rapidly becoming white, opaque conglomerates of microparticles which retain the outward "shape" of the original crystal. When an X-ray oscillation photograph of a conglomerate was taken, a powder diffraction pattern was obtained, the indexing of which indicated that the conglomerate consisted of microcrystals of Cd(CN)₂. Crystals which had degenerated in this way could not be "revived" by addition of solvent. When crystals of the butanol solvate are exposed to chloroform vapor, a "solvate exchange" process occurs (verified by IR spectroscopy); CHCl₃ is incorporated and butanol and water are lost (complete substitution within a day at room temperature). This is achieved reproducibly by placing crystals of Cd(CN)₂·²/₃H₂O·*t*-BuOH together with a little mother liquor on a porous tile inside a sealable chamber containing an atmosphere saturated with chloroform vapor above a reservoir of liquid chloroform, such that no liquid chloroform comes into contact with the tile or the crystals. The crystals retain their transparency and well-defined external form throughout the solvent exchange process. The daughter crystals are stable in the chloroform vapor-saturated atmosphere or in contact with liquid chloroform but degenerate on exposure to the atmosphere in just the same way as the parent crystals, giving conglomerates of Cd(CN)₂

[†] University of Melbourne.

[†] Australian Radiation Laboratory.

(1) Shugam, E.; Zhdanov, H. *Acta Physicochim. URSS* 1945, 20, 247.
(2) (a) Kitazawa, T.; Nishikiori, S.; Kuroda, R.; Iwamoto, T. *Chem. Lett.* 1988, 1729. (b) Kitazawa, T.; Nishikiori, S.; Yamagishi, A.; Kuroda, R.; Iwamoto, T. *J. Chem. Soc., Chem. Commun.* 1992, 413.

(3) (a) Abrahams, B. F.; Hoskins, B. F.; Robson, R. *J. Chem. Soc., Chem. Commun.* 1990, 60. (b) Abrahams, B. F.; Hoskins, B. F.; Liu, J.; Robson, R. *J. Am. Chem. Soc.* 1991, 113, 3045. (c) Kitazawa, T.; Nishikiori, S.; Kuroda, R.; Iwamoto, T. *Chem. Lett.* 1988, 459. (d) Iwamoto, T. *Inclusion Compounds*; Atwood, J. L., Davies, J. E. D., MacNicol, D. D., Eds.; Academic Press: London 1984; Vol. 1, Chapter 2.

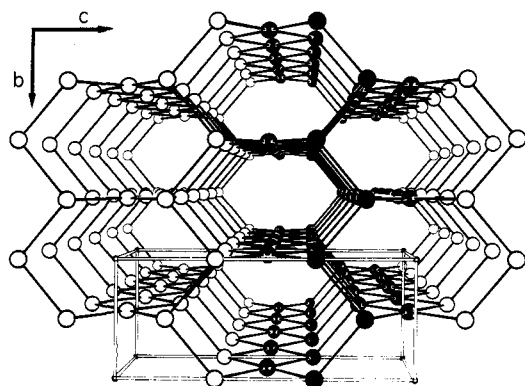


Figure 1. Perspective view down the *a* axis of the framework structure of $\text{Cd}(\text{CN})_2 \cdot \frac{2}{3}\text{H}_2\text{O} \cdot t\text{-BuOH}$ showing only the Cd centers. The orthorhombic unit cell is indicated. Cd's which appear square planar are in fact octahedral with two trans-coordinated H_2O s, omitted here for clarity. The hexagonal channels are occupied by disordered *t*-BuOH. Shaded atoms highlight one otto slab (see text) with diamond-like connectivity.

microcrystals; the degenerated crystals could not be "revived" by addition of chloroform. X-ray structural analysis of a thus-formed chloroform-solvated crystal sealed with liquid CHCl_3 in a Lindemann glass tube revealed that not only had the single-crystal character been retained but, to our astonishment, the $[\text{Cd}(\text{CN})_2]_n$ framework had undergone large-scale reorganization to generate a single diamond-like framework with chloroform in the interstices; an orthorhombic crystal had become a cubic crystal. The X-ray study⁴ revealed a face-centered cubic unit cell with $a = 12.638$ (3) Å and a structure isomorphous to that reported by Iwamoto for $\text{Cd}(\text{CN})_2 \cdot \text{CCl}_4$ with $a = 12.668$ (2) Å^{2a} (recently revised to 12.714 (1) Å^{2b}). Examination by polarized light microscopy indicated that the CHCl_3 -solvated crystals were isotropic,⁵ which is consistent with the cubic nature of the crystals.

The chloroform-solvated crystals are very similar in external appearance to the individual *tert*-butyl alcohol crystals from which they are formed. Indexing of faces reveals that one of the cubic axes of the product coincides with the *c* axis of the orthorhombic starting crystal and the other two cubic axes are at 45° to the *a* and *b* orthorhombic axes.

We note that slabs of the honeycomb structure, one of which is indicated by the shaded atoms in Figure 1, have an identical $[\text{Cd}(\text{CN})_2]_n$ topology and a geometry almost identical to those of slabs of the diamond framework in the chloroform-solvated crystal. Moreover, the axes of the cubic diamond-like framework to which these slabs of honeycomb belong are oriented relative to the orthorhombic axes of the honeycomb in precisely the manner observed experimentally for the honeycomb to diamond transformation, viz., one cubic axis, which we shall call *c*, coincident with the *c* orthorhombic axis and the other two at 45° to the *a* and *b* orthorhombic axes. We suspect these relationships are no coincidence and that they afford considerable insight into the nature of the transformation.

(4) Crystal data: $\text{Cd}(\text{CN})_2 \cdot \text{CHCl}_3$, $M = 283.8$; cubic, space group $Fd\bar{3}m$; $a = 12.638$ (3) Å; $U = 2019$ (1) Å³; $Z = 8$; $D_c = 1.868$ g cm⁻³; μ (Mo $K\alpha$) = 28.25 cm⁻¹; $F(000) = 1056$. Integrated intensity data were collected with an Enraf-Nonius CAD-4F diffractometer equipped with Mo $K\alpha$ radiation (graphite crystal monochromator) employing the $\omega/2\theta$ scan method. The structure was solved by a combination of Patterson and difference Fourier syntheses. Full-matrix least-squares refinements were employed. Weak diffraction data together with highly disordered chloroform molecules within the large adamantane-like cavities limited the precision of the structure. At convergence, $R = 0.137$ for 65 unique reflections [$I \geq 3\sigma(I)$]. A typical width of a reflection peak as determined by the Enraf-Nonius CAD-4F peak profile analysis method (ω -scan) is significantly greater for the CHCl_3 solvate ($\sim 0.4^\circ$) than for $\text{Cd}(\text{CN})_2 \cdot \frac{2}{3}\text{H}_2\text{O} \cdot t\text{-BuOH}$ ($\sim 0.2^\circ$). This indicates a higher degree of mosaicity for the chloroform-solvated crystal.

(5) Following a referee's suggestion, for which we are very grateful, we have observed the transformation by polarized light microscopy, which reveals that the reaction starts at the surfaces of the crystal and progresses inward at a roughly equal rate so that at intermediate stages an inner unchanged region can be seen with an outline very similar in shape to the outline of the crystal.

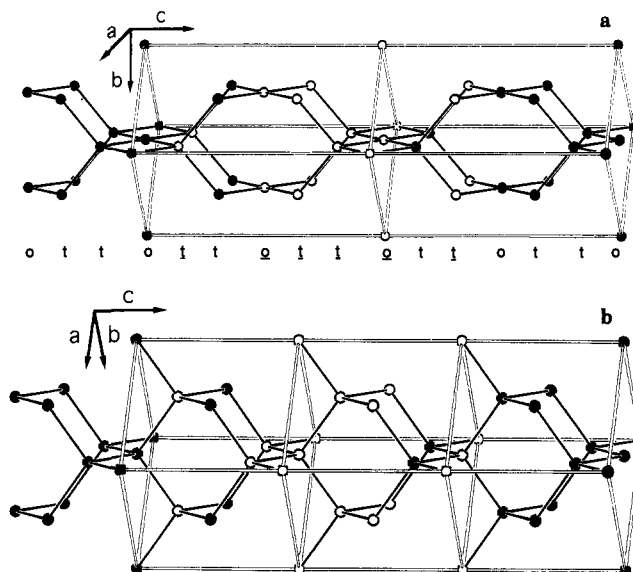


Figure 2. (a) Two "extended" cells of $\text{Cd}(\text{CN})_2 \cdot \frac{2}{3}\text{H}_2\text{O} \cdot t\text{-BuOH}$, each with the same *c* dimension as the true orthorhombic unit cell (compare Figure 1) but with twice the volume. The axes indicated refer to the orthorhombic unit cell. Sheets of shaded atoms do not require sliding to adopt positions appropriate to the diamond framework shown in b. (b) Three cubic unit cells of the diamond-like chloroform solvate (Cd centers only). The positions of shaded atoms here are to be compared with those in a.

All of the Cd's in both the honeycomb and the diamond frameworks fall into sheets parallel to *ab*, hereafter referred to as "ab sheets". In the diamond structure, these sheets consist of a simple square grid of Cd's (Cd...Cd, 8.96 Å); in the honeycomb the arrangement is distorted from square to rectangular (Cd...Cd, 8.69 and 8.55 Å) and is the same for sheets of octahedral Cd's (o sheets) as for sheets of tetrahedral Cd's (t sheets).

In the honeycomb the sequence of ab sheets is ...ottottottotto... with six sheets per repeat unit of 21.09 Å along *c* as can be seen in Figure 1, which also reveals that the diamond-like slabs involve four adjacent sheets of the type otto.

Consideration of models reveals that it is possible to convert the honeycomb disposition of Cd's (temporarily setting aside the cyanides) into the diamond disposition merely by sliding the sheets underlined in the sequence ...[otto]t[otto]t[otto]t[otto]t... relative to the rest, along half a diagonal of a Cd_4 ab rectangle. The patterns of underlined and nonunderlined groups are identical, and indeed the groups are equivalent. Relative movements within either the underlined set or the nonunderlined set are not required, so that the original diamond-like connectivities present in all of the [otto] groups need not be disrupted, and they are bracketed above for this reason. Within each of these [otto] groups there are three sheets of cyanides whose connectivities to Cd's are conserved, but between [otto] groups in regions such as ...[otto](CN)_xt(CN)_xt(CN)_x[otto]... there are three sheets of cyanides where Cd-cyanide bond breaking and making must accompany the shearing. Models suggest that in these regions no more than two of the four links to any Cd need be broken.

Figure 2 presents a "before and after" view of this hypothetical shearing process in terms of the Cd dispositions within a chosen 3D region in which we have arbitrarily "fixed" one group of sheets (shaded), so that the unshaded ones are the sheets that move. Two of the enlarged honeycomb cells shown in Figure 2a aligned along *c*, each containing six ab sheets and twelve Cd's, are thereby transformed into three cubic diamond cells shown in Figure 2b, each containing four ab sheets and eight Cd's. This hypothetical shearing process accounts in an appealing way for the transformation and for the observed relationships between axes; devising experimental procedures to probe the mechanism, however, presents a challenge.

Although this transformation shows similarities to a number of solid-state reactions, some of long-standing interest,⁶ we are

